



Influence of airmass transport events on the variability of surface ozone

J. Ma et al.

Influence of airmass transport events on the variability of surface ozone at Xianggelila Regional Atmosphere Background Station, Southwest China

J. Ma^{1,*}, W. L. Lin^{1,2}, X. D. Zheng¹, X. B. Xu¹, Z. Li³, and L. L. Yang³

¹Key Laboratory for Atmospheric Chemistry, Chinese Academy of Meteorological Sciences, Beijing 100081, China

²Centre for Atmosphere Watch and Services, Meteorological Observation Centre, China Meteorological Administration, Beijing 100081, China

³Yunnan Diqing Meteorological Bureau, Diqing 674400, China

* now at: Atmospheric Research Center, Fok Ying Tung Graduate School, Hong Kong University of Science and Technology, Hong Kong

Received: 13 November 2013 – Accepted: 2 January 2014 – Published: 21 January 2014

Correspondence to: W. L. Lin (linwl@cams.cma.gov.cn)

Published by Copernicus Publications on behalf of the European Geosciences Union.

Title Page	
Abstract	Introduction
Conclusions	References
Tables	Figures
⏪	⏩
◀	▶
Back	Close
Full Screen / Esc	
Printer-friendly Version	
Interactive Discussion	



Influence of airmass transport events on the variability of surface ozone

J. Ma et al.

Title Page

Abstract

Introduction

Conclusions

References

Tables

Figures

⏪

⏩

◀

▶

Back

Close

Full Screen / Esc

Printer-friendly Version

Interactive Discussion

Danielsen, 1968). Although the chemical production is regarded as a main source of tropospheric O_3 (Fishman et al., 1979; Gidel and Shapiro, 1980), the influence of O_3 transported from stratosphere is considerable at some remote background sites where regional and local emissions of O_3 precursors are extremely limited (Ordóñez et al., 2007; Trickl et al., 2010; Logan et al., 2012; Oltmans et al., 2012; Parrish et al., 2012). Due to the stratosphere-to-troposphere exchange and the distance from the Earth surface, where sources of trace species are located, air in upper troposphere often shows unique chemical signature. Aircraft measurements show that the climatological levels of O_3 , CO, and H_2O in the upper troposphere and lower stratosphere (UTLS) over the subtropics of the Northern Hemisphere are respectively in the ranges of 80–160 ppb, 50–85 ppb, and 6–40 ppm, depending on season (Tilmes et al., 2010). Therefore, transport events of air-masses associated with stratospheric intrusions were usually characterized by high O_3 , but low CO and water vapor concentrations (Marenco et al., 1998; Bonasoni et al., 2000; Stohl et al., 2000; Cooper et al., 2002; Langford et al., 2009; Neuman et al., 2012;). Such transport events often associated with tropopause folding synoptic systems in the middle latitudes such as cold fronts in the lower troposphere (Stohl and Trickl, 1999), corresponding with troughs/cut-off lows in the middle and upper troposphere (Davies and Schuepbach, 1994).

Tibetan Plateau is a unique topography owing to its high average elevation in excess of 4000 m a.s.l. and huge area (about 3 000 000 km²). The kinetics and thermodynamics on the unique topography have great impacts on air circulations, climate changes, in local, regional or even global scales. It is important to understand the influence of transport events from upper troposphere and lower stratosphere, which may represent one of the most important natural inputs of tropospheric O_3 and impact the atmospheric radiative forcing in the Tibetan Plateau. Moore and Semple (2005) reported the existence of so called the Tibetan “Taylor Cap” and a halo of stratospheric O_3 over the Himalaya, which causes elevated levels of the upper tropospheric O_3 along the mountain regions. This result strongly suggests that the topography of the Tibetan Plateau can exert an influence on the lower-stratosphere and upper-troposphere. So far, surface O_3 mea-

Influence of airmass transport events on the variability of surface ozone

J. Ma et al.

Title Page

Abstract

Introduction

Conclusions

References

Tables

Figures

⏪

⏩

◀

▶

Back

Close

Full Screen / Esc

Printer-friendly Version

Interactive Discussion

5 surements in the Tibetan Plateau have been reported mainly for the Waliguan global WMO/GAW station (36.28° N, 100.90° E, 3816 ma.s.l.) in the north-eastern plateau since 1994 (Tang et al., 1995; Klausen et al., 2003; Wang et al., 2006; Xu et al., 2011) and, on the south rim of the Himalaya, the Nepal Climate Observatory-Pyramid (NCO-P, 27.95° N, 86.80° E, 5079 ma.s.l.) (Cristofanelli et al., 2010). At Waliguan, high-O₃ events were mostly observed when transport events of the upper troposphere–lower stratosphere air occurred in spring (Ding and Wang, 2006; Zheng et al., 2011), and the summertime O₃ peak was deemed to be under the great influence of vertical mixing process including the stratosphere-troposphere exchange (Ma et al., 2002, 2005; Zheng et al., 2005; Liang et al., 2008). Based on the measurements at NCO-P, Cristofanelli et al. (2010) reported an assessment of the influence of stratospheric intrusions (SI) on surface O₃ and concluded that 14.1% of analyzed days were found to be affected by SI during a 2 yr investigation.

15 In this paper, we present 2 yr (from December 2007 to November 2009) measurements of surface O₃ and CO at the Xianggelila station, which located at the southeast rim of the Tibetan Plateau in Southwest China. Firstly, we give general introduction of the study including the description of observation sites, measurements of O₃ and CO, and the methods of analysis. Then, we summarize the seasonal variations of O₃ and CO, and show the main patterns of airflow which may influence the Xianggelila site. We study the impacts of downward transport on surface O₃ using a normalized indicator of transport events, which is less influenced by seasonality of trace species. In addition, we show analysis results of backward trajectories combined with the surface measurement data and demonstrate a case of O₃ transport event caused by a deep westerly trough. Finally, the influence of airmass transport events from the upper O₃-rich atmosphere on the surface O₃ is assessed using the chemical tracers.

20

25

2 Measurements and methodologies

2.1 Overview of the Xianggelila station

The Xianggelila Regional Atmospheric Background Station (28.006° N, 99.726° E, 3580 m.a.s.l.) is located in Yunnan province, Southwest China (Fig. 1), and is one of the background stations operated by China Meteorological Administration (CMA). The station is at the southeast rim of the Tibetan Plateau and about 450 km northwest of Kunming City (population about 7.263 millions in 2011), the capital of Yunnan province. It is considered to be weakly affected by the local anthropogenic activities because there is nearly no significant anthropogenic source of O₃ precursors surrounding the station, and the nearest township, Xianggelila County, is about 30 km away from the station. Hence, it is regarded as an ideal site to monitor the background levels of trace gases in the atmosphere over Southwest China. The climatology of Xianggelila is mainly controlled by monsoon activities. The Asian summer monsoon can bring abundant precipitation there.

2.2 Measurements of O₃ and CO

A set of commercial instruments from Ecotech, Australia has been used to measure O₃ (9810B) and CO (9830T) at the Xianggelila station. The air inlet is fixed at the height of 1.8 m above the roof of the building and about 8 m above the ground. The common inlet and all other tubing are made of Teflon. Weekly zero/span checks were done using a dynamic gas calibrator (Gascal 1100) in combination with a zero air supply (8301LC) and a set of standard reference gas mixtures (National Institute of Metrology, Beijing, China). Additional CO-free air was also produced using SOFNOCAT (514) oxidation catalysts (www.molecularproducts.com) and supplied to the CO analyzer every 2 h for additional auto-zero (background) cycles. Multi-point calibrations of the CO analyzers were made every month. The national CO standard gas was compared against the NIST-traceable standard from Scott Specialty Gases, USA. Multi-point calibrations of

Influence of airmass transport events on the variability of surface ozone

J. Ma et al.

Title Page

Abstract

Introduction

Conclusions

References

Tables

Figures



Back

Close

Full Screen / Esc

Printer-friendly Version

Interactive Discussion



Influence of airmass transport events on the variability of surface ozone

J. Ma et al.

Title Page

Abstract

Introduction

Conclusions

References

Tables

Figures

⏪

⏩

◀

▶

Back

Close

Full Screen / Esc

Printer-friendly Version

Interactive Discussion

the O₃ analyzer were made every month using an O₃ calibrator (TE 49i PS), which is traceable to the Standard Reference Photometer (SRP) maintained by WMO World Calibration Centre in Switzerland (EMPA). Measurement signals were recorded as 1 min averages. After the correction of data on the basis of the results of the multi-point calibrations and zero/span checks, hourly average concentrations were calculated and are used for further analysis. Meteorological data, including wind, temperature, relative humidity, etc., were also obtained from the site, with a resolution of 1 h.

2.3 Backward-trajectory calculation and weather simulation

The HYSPLIT (Hybrid Single-Particle Lagrangian Integrated Trajectory, version 4.8) model was used to calculate the backward trajectories at Xianggelila from 2007 to 2009. The HYSPLIT model is a complete system for computing simple air parcel trajectories to complex dispersion and deposition simulations (Draxler and Rolph, 2003; Rolph, 2010). National Centers for Environmental Prediction (NCEP, 1° × 1°) reanalysis meteorological data were inputted for model calculation. The vertical motion method in the calculations is the default model selection, which uses the meteorological model's vertical velocity fields and is terrain following. The height of endpoint is set at 500 m above ground level for characterizing the airmass transport patterns in the free atmosphere. The 3 day backward trajectories were calculated at four times (00:00, 06:00, 12:00, 18:00 UTC) per day. After calculation, the trajectories were clustered into several types using the HYSPLIT software. Besides, HYSPLIT is also used to calculate 7 day backward trajectories in the case study (see Sect. 3.3).

The Weather Research and Forecasting (WRF) Model Version 3.4.1 (Skamarock et al., 2005) is used to simulate the weather situations in Sect. 3.3 for a case study. Only one domain was initialized by NCEP FNL (Final) Operational Global Analysis data on 1.0° × 1.0° grids prepared operationally every six hours, and the space resolution of WRF is set to 36 km. The run time of WRF was set as two days and used default physical schemes.

physical process of transport events is assumed by the Y indicator, and this is inevitably influenced by the photochemical processes of O_3 and CO. Under situations when the physical processes are much more dominant than the local photochemical production in source of surface O_3 , the Y indicator is expected to act as a good tracer.

3 Results and discussion

3.1 Seasonal and diurnal variations of O_3 and CO

The monthly averaged O_3 and CO are shown in Table 1. Both O_3 and CO reached maxima in spring (O_3 : 55.2 ± 9.3 ppb, CO: 183 ± 57 ppb), and the highest monthly-averaged O_3 concentrations of 58.3 ppb appeared in April. The spring maximum of O_3 at Xianggelila is consistent with the observations elsewhere in the Northern Hemisphere (Monks et al., 2000). In winter, the concentration of CO is low, but the concentration of O_3 is still relatively high with an average level of 45.8 ppb. On the contrary, in summer and fall, O_3 level is low, but CO remains relatively high level.

Table 1 also shows the maxima and minima of the average diurnal variation of O_3 in different months. The average diurnal variation of O_3 at Xianggelila maximizes in the early afternoon (12:00–14:00 LT) and minimizes in the early morning. This diurnal ozone pattern seems very similar with the typical diurnal O_3 pattern in urban or polluted area, at which photochemical product of O_3 can accumulated after the noon. However, at Xianggelila, the peak O_3 at daytime is strongly associated with the wind speed, as showed in Fig. 2. In the early morning, O_3 mixing ratios increase sharply with the increase of wind speed. During the high-wind-speed period (12:00–16:00 LT), O_3 maintains high levels, and then O_3 decreases with the decrease of wind speed till the night. Strong wind is not conducive to the accumulation of the local photochemical production of O_3 and it also can force O_3 losses by processes like deposition. Therefore, the transport and deposition will be the key factors than local photochemical process influencing the diurnal variations of surface O_3 at Xianggelila, a remote and clean site.

Influence of airmass transport events on the variability of surface ozone

J. Ma et al.

Title Page

Abstract

Introduction

Conclusions

References

Tables

Figures

⏪

⏩

◀

▶

Back

Close

Full Screen / Esc

Printer-friendly Version

Interactive Discussion



Influence of airmass transport events on the variability of surface ozone

J. Ma et al.

Title Page

Abstract

Introduction

Conclusions

References

Tables

Figures

◀

▶

◀

▶

Back

Close

Full Screen / Esc

Printer-friendly Version

Interactive Discussion



The maximal amplitude of the diurnal variation of O_3 was found in spring, and the minimal in winter. In monsoon season, the lowest diurnal amplitude was found in August (14.5 ppb, smaller than that in June, July, and September). In August, the precipitation and cloud coverage reached the annual maximum and the mixing layer height reached the minimum (Fig. 3). The boundary mixing layer height is calculated using the surface meteorological data according to the method proposed by Cheng et al. (2001). The cloud may decrease the solar radiation and weaken the mixing ability between free atmosphere and surface. The precipitation can remove more O_3 and its precursors from the troposphere. These factors together contribute significantly to the low level of the average surface O_3 and the smaller diurnal amplitude of O_3 in monsoon season, especially in August.

3.2 Trajectory and surface measurements

3-day airmass backward trajectories during the measurement period were calculated for every 6 h, and then clustered into 7 clusters. The mean trajectory for each cluster, the ratios, and their patterns are shown in Fig. 4. The average temperature, water vapor, O_3 , and CO corresponding to each type of cluster are listed in Table 2. The dominant clusters are type 6 (55.1 %), type 5 (28.1 %) and type 7 (7.3 %), with low level trajectory heights and relatively high CO level over 135 ppb. Types 5–7 can be recognized as relatively polluted clusters. O_3 in types 6 and 7 is lowest, because these types of trajectories occur mainly in summer and fall, when Xianggelila is influenced by monsoon and abundant rains, which inhibit the photochemical accumulation of O_3 . O_3 in type 5 is 44.8 ppb, a relatively high level and this type of trajectories mostly occur in spring and winter with less rains. Trajectories of types 1–4 are with high transport height and low CO, so they can be recognized as cleaner types in terms of CO. However, O_3 in types 1–4 is relatively high, indicating that these types of trajectories possibly carry O_3 -rich airmass from free troposphere to surface. Types 1–4 mainly occur in winter, spring and fall, and very rare in summer.

Influence of airmass transport events on the variability of surface ozone

J. Ma et al.

Title Page

Abstract

Introduction

Conclusions

References

Tables

Figures

⏪

⏩

◀

▶

Back

Close

Full Screen / Esc

Printer-friendly Version

Interactive Discussion

Figure 5 shows kernel density of trajectory pressure levels (the minimal one during 72 h backward trajectories), trajectory height (the maximal one during 72 h backward trajectories) and hourly Y indicator. In summer, trajectories are most likely to travel very low with high pressure levels, and smallest Y indicators are observed. The spring kernel density of trajectory resembles that in fall, but Y indicator in spring has lower possibility in the range of Y value between 3 and 7 than that in fall. This reflects that the Y indicator is able to indicate the different behavior of O_3 in different season. It is intriguing that the kernel density of trajectories in winter has a peak between 200 and 500 hPa, and accordingly, the density of Y indicator is much higher in winter than in other seasons. This is consistent with the seasonality of the subtropical jet (Sprenger and Wernli, 2003; Sprenger et al., 2003) and with the seasonal cycle of deep stratospheric intrusions over Central Europe (Trickl et al., 2010). The high possibility of low trajectory pressure level and the high Y value in winter implies the high possibility of ozone transport events in winter. In spring and fall, small peaks of the kernel density of trajectory pressure level and height are also obvious around the low pressure level at about 200 hPa to 400 hPa or high height at 1000 m to 3000 m, but the possibility is much lower than that in winter. What is intriguing is that the possibility of low trajectory pressure levels and high heights is a little higher in spring than in fall, but the possibility of large Y indicator is higher in fall than in spring. This reverse behavior of trajectory and Y indicator in spring and fall might imply that transport events from high altitudes does not necessarily enhance the O_3 level and its variation, especially in spring when photochemical production might be a significant source of O_3 . It should be noted that there exists a tiny peak of kernel probability density of pressure around 430 hPa, height around 4800 m and Y indicator around 8 in summer. This is due to a strong ozone transport event and will be discussed in Sect. 3.3.

Figure 6 shows the trajectory pressure level (or height a.g.l.) and the Y indicator in each month with their correlation coefficients and significance levels (P values). The seasonal variation of Y indicator shows a maximum in winter (2.5 to 3.0), a slight downward trend from spring to fall (1.5 to 2.0), and reached the lowest level (< 1.5) in

down the O₃-rich air with less water vapor and CO into the troposphere and influenced the surface.

3.4 Estimation of the frequency of transport events

As discussed in Sect. 3.3, Y indicator can be used to indicate O₃ transport events. A transport event might last at a high-lying surface site for several or dozens of hours. So, if Y indicator keeps at a relatively high level for several consecutive hours or days, there may have the possibility of O₃ transport events.

There are totally 784 h with Y higher than 3, and the times of consecutive day with Y higher than 3, 4, and 5 are 200, 136, and 91, respectively, as shown in Table 3. The numbers of consecutive days with Y higher than 8 are 15 in winter, 12 in fall, 4 in spring and summer, indicating that the Y value-deduced occurrence of transport events vary largely from season to season. The transport events occur most frequently in winter, followed in fall, spring and the least in summer. To further analyze the frequency of the transport events, the relationship between the trajectory pressure level and Y is analyzed. The numbers of hours with both Y higher than a given value and trajectory pressure level lower than a given level are calculated for each season and shown in Fig. 11. In summer, hours with both low trajectory pressure levels and high Y values were rare, and this coincides with to the minimal O₃ mixing ratio in summer. In summer monsoon season, there were about 68.7% of days with precipitation at Xi-angelila, which inhibits the accumulation of O₃. The average trajectory height (only average maximal height during 72 h) in summer was extremely low (134 m ending at 500 m a.g.l.), which limited the exchange of surface air with the upper free troposphere. In winter, the number of hours with both Y higher than 2 and trajectory pressure level lower than 500 hPa is nearly 2400 h. The trajectory pressure in winter was significantly lower, indicating relatively higher O₃ from upper atmosphere to contribute the surface O₃ budget (Lefohn et al., 2001). The possibility of O₃ transport events in fall was also high with a wide range of trajectory over 1000 m and Y over 3. Together with Table 2, it

Influence of airmass transport events on the variability of surface ozone

J. Ma et al.

Title Page

Abstract

Introduction

Conclusions

References

Tables

Figures



Back

Close

Full Screen / Esc

Printer-friendly Version

Interactive Discussion

Influence of airmass transport events on the variability of surface ozone

J. Ma et al.

Title Page

Abstract

Introduction

Conclusions

References

Tables

Figures

⏪

⏩

◀

▶

Back

Close

Full Screen / Esc

Printer-friendly Version

Interactive Discussion

Although Y indicator can be used to study the influence of transport events from the upper O_3 -rich atmosphere and obtain qualitative or semi-quantitative results, there are still questions needed to be answered like what is the criterion of Y indicator to indicate what a height for transport events. Table 4 shows the monthly results of the O_3 –CO correlations, derived from 10:00–18:00 LT measurements from Xianggelila. The correlations are statistically significant from February to November. Relatively steep negative slopes are found in May, June, September, October, November and a flatter negative slope in December, suggesting that there are clear influences from the upper troposphere and lower stratospheric air masses in these months. Significant positive O_3 –CO correlations with steeper slopes are found in July, August, February, March and April, which indicate that the influences of photochemical production of O_3 are probably more important in these months.

4 Conclusions

A two-year measurement of surface O_3 and CO was made from December 2007 to November 2009 at Xianggelila in Southwest China. The maximal O_3 and CO mixing ratios were observed in spring, followed in winter and fall, and the minima was in summer. According to the analysis of backward trajectories, Xianggelila was influenced largely by the high and fast airflows from the south or north Tibet-Plateau in winter, fall and spring. In summer, trajectories to Xianggelila were mainly from the south and east regions, and their moving heights were very low under the influence of Asian Monsoon from the end of May to the end of September. As a result, the minimal O_3 was found in summer due to the most frequent precipitation and cloudiness, and the CO level in summer kept at a relatively high level because of the air transport from the south and east regions with intense anthropogenic CO emissions. The CO level was low in winter because of the airmasses originated partly from the relatively clean Tibetan Plateau.

A transport indicator (Y), which combined the measured data of the chemical tracers of O_3 , CO, and water vapor is proposed to indicate the fluctuation of O_3 and sources

Influence of airmass transport events on the variability of surface ozone

J. Ma et al.

Title Page

Abstract

Introduction

Conclusions

References

Tables

Figures

◀

▶

◀

▶

Back

Close

Full Screen / Esc

Printer-friendly Version

Interactive Discussion



- Cooper, O., Moody, J., Parrish, D., Trainer, M., Holloway, J., Hübler, G., Fehsenfeld, F., and Stohl, A.: Trace gas composition of midlatitude cyclones over the western North Atlantic Ocean: a seasonal comparison of O₃ and CO, *J. Geophys. Res.*, 107, 4057, doi:10.1029/2001JD000902, 2002.
- 5 Cristofanelli, P., Calzolari, F., Bonafè, U., Duchi, R., Marinoni, A., Roccato, F., Tositti, L., and Bonasoni, P.: Stratospheric intrusion index (SI²) from baseline measurement data, *Theor. Appl. Climatol.*, 97, 317–325, 2009.
- Cristofanelli, P., Bracci, A., Sprenger, M., Marinoni, A., Bonafè, U., Calzolari, F., Duchi, R., Laj, P., Pichon, J. M., Roccato, F., Venzac, H., Vuillermoz, E., and Bonasoni, P.: Tropo-
10 spheric ozone variations at the Nepal Climate Observatory-Pyramid (Himalayas, 5079 m a.s.l.) and influence of deep stratospheric intrusion events, *Atmos. Chem. Phys.*, 10, 6537–6549, doi:10.5194/acp-10-6537-2010, 2010.
- Crutzen, P. J.: Photochemical reactions initiated by and influencing ozone in unpolluted tropospheric air, *Tellus*, 26, 47–57, 1974.
- 15 Crutzen, P. J., Lawrence, M. G., and Pöschl, U.: On the background photochemistry of tropospheric ozone, *Tellus B*, 51, 123–146, 1999.
- Danielsen, E. F.: Stratospheric-tropospheric exchange based on radioactivity, ozone and potential vorticity, *J. Atmos. Sci.*, 25, 502–518, 1968.
- Davies, T. and Schuepbach, E.: Episodes of high ozone concentrations at the earth's surface
20 resulting from transport down from the upper troposphere/lower stratosphere: a review and case studies, *Atmos. Environ.*, 28, 53–68, 1994.
- Ding, A. and Wang, T.: Influence of stratosphere-to-troposphere exchange on the seasonal cycle of surface ozone at Mount Waliguan in western China, *Geophys. Res. Lett.*, 33, L03803, doi:10.1029/2005GL024760, 2006.
- 25 Draxler, R. and Rolph, G.: HYSPLIT (HYbrid Single-Particle Lagrangian Integrated Trajectory) model, available at: <http://www.arl.noaa.gov/ready/hysplit4.html> (last access: 4 December 2013), NOAA Air Resources Laboratory, Silver Spring, MD, 2003.
- Fishman, J., Solomon, S., and Crutzen, P. J.: Observational and theoretical evidence in support of a significant in-situ photochemical source of tropospheric ozone, *Tellus*, 31, 432–446,
30 1979.
- Gidel, L. T. and Shapiro, M.: General circulation model estimates of the net vertical flux of ozone in the lower stratosphere and the implications for the tropospheric ozone budget, *J. Geophys. Res.*, 85, 4049–4058, 1980.

Influence of airmass transport events on the variability of surface ozone

J. Ma et al.

Title Page

Abstract

Introduction

Conclusions

References

Tables

Figures

⏪

⏩

◀

▶

Back

Close

Full Screen / Esc

Printer-friendly Version

Interactive Discussion

- He, Y. J., Uno, I., Wang, Z. F., Pochanart, P., Li, J., and Akimoto, H.: Significant impact of the East Asia monsoon on ozone seasonal behavior in the boundary layer of Eastern China and the west Pacific region, *Atmos. Chem. Phys.*, 8, 7543–7555, doi:10.5194/acp-8-7543-2008, 2008.
- 5 Hough, A. M. and Derwent, R. G.: Changes in the global concentration of tropospheric ozone due to human activities, *Nature*, 344, 645–648, 1990.
- Jacob, D. J.: Heterogeneous chemistry and tropospheric ozone, *Atmos. Environ.*, 34, 2131–2159, 2000.
- Jain, S., Arya, B., Kumar, A., Ghude, S. D., and Kulkarni, P.: Observational study of surface ozone at New Delhi, India, *Int. J. Remote Sens.*, 26, 3515–3524, 2005.
- 10 Junge, C. E.: Global ozone budget and exchange between stratosphere and troposphere, *Tellus*, 14, 363–377, 1962.
- Klausen, J., Zellweger, C., Buchmann, B., and Hofer, P.: Uncertainty and bias of surface ozone measurements at selected Global Atmosphere Watch sites, *J. Geophys. Res.*, 108, 4622, doi:10.1029/2003JD003710, 2003.
- 15 Krupa, S. V. and Manning, W. J.: Atmospheric ozone: formation and effects on vegetation, *Environ. Pollut.*, 50, 101–137, 1988.
- Lefohn, A. S., Oltmans, S. J., Dann, T., and Singh, H. B.: Present-day variability of background ozone in the lower troposphere, *J. Geophys. Res.*, 106, 9945–9958, 2001.
- 20 Liang, M. C., Tang, J., Chan, C. Y., Zheng, X., and Yung, Y. L.: Signature of stratospheric air at the Tibetan Plateau, *Geophys. Res. Lett.*, 35, L20816, doi:10.1029/2008GL035246, 2008.
- Logan, J., Staehelin, J., Megretskaia, I., Cammas, J. P., Thouret, V., Claude, H., De Backer, H., Steinbacher, M., Scheel, H. E., and Stübi, R.: Changes in ozone over Europe: analysis of ozone measurements from sondes, regular aircraft (MOZAIC) and alpine surface sites, *J. Geophys. Res.-Atmos.*, 117, D09301, doi:10.1029/2011JD016952, 2012.
- 25 Ma, J., Zhou, X., and Hauglustaine, D.: Summertime tropospheric ozone over China simulated with a regional chemical transport model, 2. Source contributions and budget, *J. Geophys. Res.-Atmos.*, 107, ACH2-1–ACH2-11, 2002.
- Ma, J., Zheng, X. D., and Xu, X. D.: Comment on “Why does surface ozone peak in summertime at Wa Liguan?” by Bin Zhu et al., *Geophys. Res. Lett.*, 32, L01805, doi:10.1029/2004GL021683, 2005.
- 30 Marengo, A., Thouret, V., Nédélec, P., Smit, H., Helten, M., Kley, D., Karcher, F., Simon, P., Law, K., and Pyle, J.: Measurement of ozone and water vapor by Airbus in-service aircraft:

Influence of airmass transport events on the variability of surface ozone

J. Ma et al.

Title Page

Abstract

Introduction

Conclusions

References

Tables

Figures

◀

▶

◀

▶

Back

Close

Full Screen / Esc

Printer-friendly Version

Interactive Discussion

the MOZAIC airborne program, an overview, *J. Geophys. Res.-Atmos.*, 103, 25631–25642, 1998.

Monks, P. S.: A review of the observations and origins of the spring ozone maximum, *Atmos. Environ.*, 34, 3545–3561, 2000.

5 Moore, G. and Semple, J. L.: A Tibetan Taylor Cap and a halo of stratospheric ozone over the Himalaya, *Geophys. Res. Lett.*, 32, L21810, doi:10.1029/2005GL024186, 2005.

Naja, M. and Lal, S.: Changes in surface ozone amount and its diurnal and seasonal patterns, from 1954–55 to 1991–93, measured at Ahmedabad (23 N), India, *Geophys. Res. Lett.*, 23, 81–84, 1996.

10 Neuman, J., Trainer, M., Aikin, K., Angevine, W., Brioude, J., Brown, S., de Gouw, J., Dube, W., Flynn, J., and Graus, M.: Observations of ozone transport from the free troposphere to the Los Angeles basin, *J. Geophys. Res.*, 117, D00V09, doi:10.1029/2011JD016919, 2012.

Ordóñez, C., Brunner, D., Staehelin, J., Hadjinicolaou, P., Pyle, J., Jonas, M., Wernli, H., and Prévôt, A.: Strong influence of lowermost stratospheric ozone on lower tropo-
spheric background ozone changes over Europe, *Geophys. Res. Lett.*, 34, L07805,
doi:10.1029/2006GL029113, 2007.

Oltmans, S., Lefohn, A., Shadwick, D., Harris, J., Scheel, H., Galbally, I., Tarasick, D., Johnson, B., Brunke, E.-G., and Claude, H.: Recent tropospheric ozone changes – a pattern dominated by slow or no growth, *Atmos. Environ.*, 67, 331–351, 2012.

20 Parrish, D. D., Law, K. S., Staehelin, J., Derwent, R., Cooper, O. R., Tanimoto, H., Volz-Thomas, A., Gilge, S., Scheel, H.-E., Steinbacher, M., and Chan, E.: Long-term changes in lower tropospheric baseline ozone concentrations at northern mid-latitudes, *Atmos. Chem. Phys.*, 12, 11485–11504, doi:10.5194/acp-12-11485-2012, 2012.

Rolph, G.: Real-time Environmental Applications and Display sYstem (READY), available at: <http://ready.arl.noaa.gov> (last access: 17 October 2013), NOAA Air Resources Laboratory, Silver Spring, MD, USA, 2010.

25 Skamarock, W. C., Klemp, J. B., Dudhia, J., Gill, D. O., Barker, D. M., Wang, W., and Powers, J. G.: A Description of the Advanced Research WRF Version 2, DTIC Document, NCAR Technical Note, NCAR/TN468+STR, 88 pp., <http://wrf-model.org/wrfadmin/publications.php>, 2005.

30 Sprenger, M. and Wernli, H.: A northern hemispheric climatology of cross-tropopause exchange for the ERA15 time period (1979–1993), *J. Geophys. Res.*, 108, 8521, doi:10.1029/2002JD002636, 2003.

Influence of airmass transport events on the variability of surface ozone

J. Ma et al.

Title Page

Abstract

Introduction

Conclusions

References

Tables

Figures

◀

▶

◀

▶

Back

Close

Full Screen / Esc

Printer-friendly Version

Interactive Discussion

Sprenger, M., Maspoli, M. C., and Wernli, H.: Tropopause folds and cross-tropopause exchange: a global investigation based upon ECMWF analyses for the time period March 2000 to February 2001, *J. Geophys. Res.*, 108, 8518, doi:10.1029/2002JD002587, 2003.

5 Staehelin, J., Harris, N., Appenzeller, C., and Eberhard, J.: Ozone trends: a review, *Rev. Geophys.*, 39, 231–290, 2001.

Stohl, A. and Trickl, T.: A textbook example of long-range transport – simultaneous observation of ozone maxima of stratospheric and North American origin in the free troposphere over Europe, *J. Geophys. Res.*, 104, 445–462, 1999.

10 Stohl, A., Spichtinger-Rakowsky, N., Bonasoni, P., Feldmann, H., Memmesheimer, M., Scheel, H., Trickl, T., Hübener, S., Ringer, W., and Mandl, M.: The influence of stratospheric intrusions on alpine ozone concentrations, *Atmos. Environ.*, 34, 1323–1354, 2000.

Tang, J., Wen, Y., Xu, X., Zheng, X., Guo, S., and Zhao, Y.: China global atmosphere watch baseline observatory and its measurement program, CAMS Annual Report 1994–1995, China Meteorology Press, Beijing, 56–65, 1995.

15 Tilmes, S., Pan, L. L., Hoor, P., Atlas, E., Avery, M. A., Campos, T., Christensen, L. E., Diskin, G. S., Gao, R.-S., Herman, R. L., Hints, E. J., Loewenstein, M., Lopez, J., Paige, M. E., Pittman, J. V., Podolske, J. R., Proffitt, M. R., Sachse, G. W., Schiller, C., Schlager, H., Smith, J., Spelten, N., Webster, C., Weinheimer, A., and Zondlo, M. A.: An aircraft-based upper troposphere lower stratosphere O₃, CO, and H₂O climatology for the Northern Hemisphere, *J. Geophys. Res.*, 115, D14303, doi:10.1029/2009JD012731, 2010.

20 Trickl, T., Feldmann, H., Kanter, H.-J., Scheel, H.-E., Sprenger, M., Stohl, A., and Wernli, H.: Forecasted deep stratospheric intrusions over Central Europe: case studies and climatologies, *Atmos. Chem. Phys.*, 10, 499–524, doi:10.5194/acp-10-499-2010, 2010.

Vaughan, G. and Price, J.: On the relation between total ozone and meteorology, *Q. J. Roy. Meteor. Soc.*, 117, 1281–1298, 1991.

25 Vingarzan, R.: A review of surface ozone background levels and trends, *Atmos. Environ.*, 38, 3431–3442, 2004.

Wang, T., Wong, H., Tang, J., Ding, A., Wu, W., and Zhang, X.: On the origin of surface ozone and reactive nitrogen observed at a remote mountain site in the north-eastern Qinghai-Tibetan Plateau, western China, *J. Geophys. Res.*, 111, D08303, doi:10.1029/2005JD006527, 2006.

30 Wang, Z. and Sassen, K.: Ozone destruction in continental stratus clouds: an aircraft case study, *J. Appl. Meteorol.*, 39, 875–886, 2000.

Influence of airmass transport events on the variability of surface ozone

J. Ma et al.

Title Page

Abstract

Introduction

Conclusions

References

Tables

Figures

◀

▶

◀

▶

Back

Close

Full Screen / Esc

Printer-friendly Version

Interactive Discussion



Xu, X., Tang, J., and Lin, W.: The trend and variability of surface ozone at the global GAW station Mt. WALIGUAN, China, in: Second Tropospheric Ozone Workshop Tropospheric Ozone Changes: Observations, State of Understanding and Model Performances, WMO/GAW report, WMO, Geneva, 49–55, 2011.

5 Zheng, X., Wan, G., Tang, J., Zhang, X., Yang, W., Lee, H., and Wang, C.: ^7Be and ^{210}Pb radioactivity and implications on sources of surface ozone at Mt. Waliguan, Chinese Sci. Bull., 50, 167–171, 2005.

10 Zheng, X., Shen, C., Wan, G., Liu, K., and Tang, J., Xu, X.: $^{10}\text{Be}/^7\text{Be}$ implies the contribution of stratosphere-troposphere transport to the winter-spring surface O_3 variation observed on the Tibetan Plateau, Chinese Sci. Bull., 56, 84–88, 2011.

Influence of airmass transport events on the variability of surface ozone

J. Ma et al.

Table 1. Monthly mean O₃ and CO, the average diurnal O₃ maxima, minima, and amplitudes.

Month	Mean ± SD	O ₃ [ppbv]			CO [ppbv] Mean ± SD
		Diurnal Max (LT)	Diurnal Min (LT)	Diurnal amplitude	
Jan	45.4 ± 5.6	49.2 (14:00)	41.4 (08:00)	7.9	139 ± 56
Feb	50.6 ± 5.8	54.3 (12:00)	47.2 (08:00)	7.1	153 ± 46
Mar	57.1 ± 6.9	61.4 (12:00)	50.5 (08:00)	10.8	185 ± 57
Apr	58.3 ± 8.8	63.7 (13:00)	50.1 (07:00)	13.6	182 ± 59
May	50.2 ± 9.8	58.4 (13:00)	39.9 (07:00)	18.5	181 ± 54
Jun	37.4 ± 11.6	46.6 (13:00)	27.9 (06:00)	18.7	146 ± 40
Jul	26.8 ± 12.5	34.8 (13:00)	18.5 (07:00)	16.3	153 ± 47
Aug	24.2 ± 8.8	31.8 (13:00)	17.3 (06:00)	14.5	156 ± 42
Sep	29.6 ± 9.2	37.7 (13:00)	20.3 (06:00)	17.4	159 ± 41
Oct	31.4 ± 10.1	37.5 (14:00)	24.1 (08:00)	13.4	124 ± 36
Nov	38.1 ± 7.8	42.8 (14:00)	33.1 (09:00)	9.7	118 ± 44
Dec	39.7 ± 5.0	44.7 (14:00)	36.1 (10:00)	8.6	119 ± 53

Title Page

Abstract

Introduction

Conclusions

References

Tables

Figures

⏪

⏩

◀

▶

Back

Close

Full Screen / Esc

Printer-friendly Version

Interactive Discussion

Influence of airmass transport events on the variability of surface ozone

J. Ma et al.

Table 2. Average air temperature ($^{\circ}\text{C}$), wind speed (ms^{-1}), specific humidity (g kg^{-1}), O_3 and CO volume mixing ratios (ppb) associated with different types of trajectories and seasonal fractioning of trajectories.

Type	T	Wind speed	humidity	O_3	CO	Spring (%)	Summer (%)	Fall (%)	Winter (%)
1	-1.9	2.8	1.5	53.5	99	50.0	0.0	0.0	50.0
2	5.0	1.8	5.0	43.8	126	38.6	18.6	17.1	25.7
3	1.6	2.1	2.1	40.5	93	4.0	0.0	28.0	68.0
4	0.9	1.9	2.4	36.0	98	10.2	0.7	21.1	68.0
5	3.2	2.3	4.2	44.8	139	46.8	2.2	17.4	33.6
6	7.1	1.9	7.9	32.6	135	17.1	37.4	28.3	17.3
7	9.5	1.6	9.7	27.6	150	14.6	49.5	35.8	0.0

Title Page

Abstract

Introduction

Conclusions

References

Tables

Figures

◀

▶

◀

▶

Back

Close

Full Screen / Esc

Printer-friendly Version

Interactive Discussion

Influence of airmass transport events on the variability of surface ozone

J. Ma et al.

Table 3. Numbers of hours and consecutive days meeting the different Y criteria.

		$Y > 3$	$Y > 4$	$Y > 5$	$Y > 6$	$Y > 7$	$Y > 8$
numbers of hours		784	396	218	138	88	72
numbers of consecutive days	ALL	200	136	91	63	46	38
	Spring	42	23	15	10	5	4
	Summer	32	14	11	9	5	4
	Fall	58	43	29	19	16	12
	Winter	65	53	32	21	17	15

Title Page

Abstract

Introduction

Conclusions

References

Tables

Figures

◀

▶

◀

▶

Back

Close

Full Screen / Esc

Printer-friendly Version

Interactive Discussion

Influence of airmass transport events on the variability of surface ozone

J. Ma et al.

Title Page

Abstract

Introduction

Conclusions

References

Tables

Figures

◀

▶

◀

▶

Back

Close

Full Screen / Esc

Printer-friendly Version

Interactive Discussion

Table 4. Monthly results of the O₃–CO correlations, derived from 10:00–18:00 LT measurements from Xianggelila. The slopes and intercepts of the regression lines were derived using the reduced-major-axis regression technique.

Month	intercept	slope	R^2	P	N
Jan	33.5	0.109	0.0007	0.59	392
Feb	35.9	0.117	0.0494	< 0.0001	438
Mar	38.7	0.119	0.1950	< 0.0001	521
Apr	39.7	0.136	0.1160	< 0.0001	519
May	83.4	−0.192	0.0531	< 0.0001	509
Jun	85.2	−0.344	0.0861	< 0.0001	516
Jul	−14.0	0.347	0.0540	< 0.0001	497
Aug	−3.1	0.233	0.0411	< 0.0001	515
Sep	67.5	−0.251	0.0547	< 0.0001	461
Oct	65.2	−0.285	0.1080	< 0.0001	499
Nov	58.4	−0.183	0.0693	< 0.0001	420
Dec	50.7	−0.094	0.0551	0.02	300

Influence of airmass transport events on the variability of surface ozone

J. Ma et al.

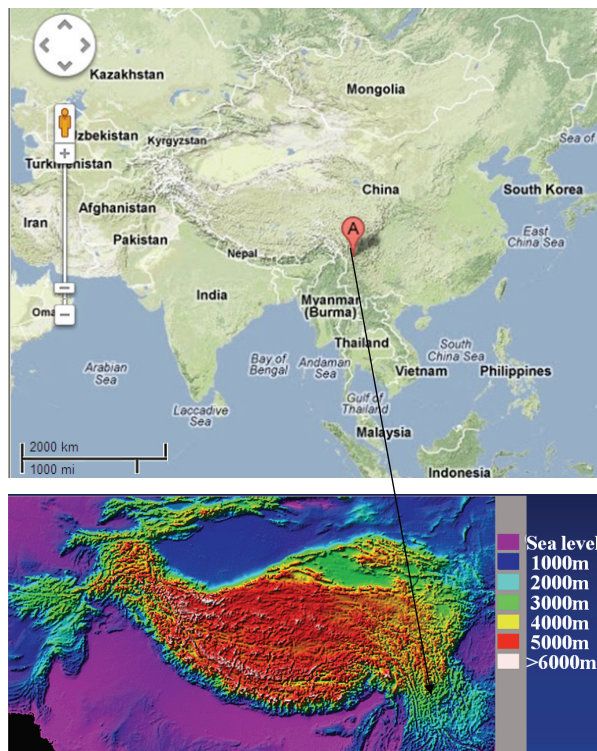


Fig. 1. The geographical location of the Xianggelila Regional Atmosphere Background Station.

Title Page	
Abstract	Introduction
Conclusions	References
Tables	Figures
⏪	⏩
⏴	⏵
Back	Close
Full Screen / Esc	
Printer-friendly Version	
Interactive Discussion	

Influence of airmass transport events on the variability of surface ozone

J. Ma et al.

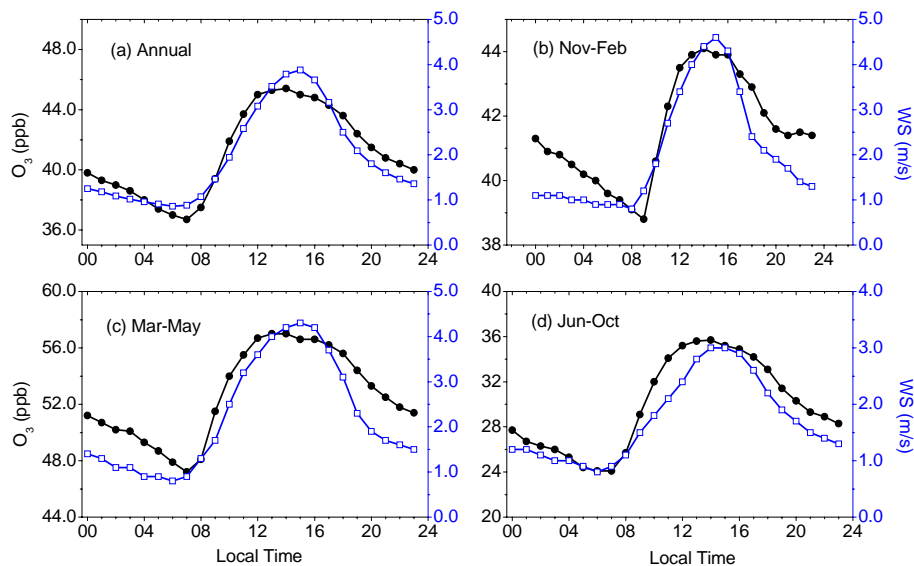


Fig. 2. The average diurnal variations of O_3 and wind speed (WS) at the Xianggelila station for different periods.

[Title Page](#)[Abstract](#)[Introduction](#)[Conclusions](#)[References](#)[Tables](#)[Figures](#)[⏪](#)[⏩](#)[⏴](#)[⏵](#)[Back](#)[Close](#)[Full Screen / Esc](#)[Printer-friendly Version](#)[Interactive Discussion](#)

Influence of airmass transport events on the variability of surface ozone

J. Ma et al.

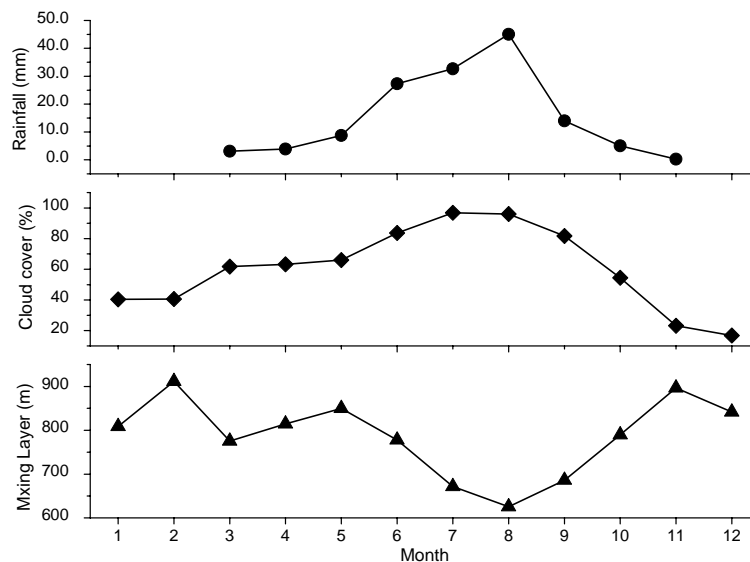


Fig. 3. Monthly variations of rainfall, cloud cover and boundary mixing layer height at Xianggelila station.

Influence of airmass transport events on the variability of surface ozone

J. Ma et al.

Title Page

Abstract

Introduction

Conclusions

References

Tables

Figures

◀

▶

◀

▶

Back

Close

Full Screen / Esc

Printer-friendly Version

Interactive Discussion

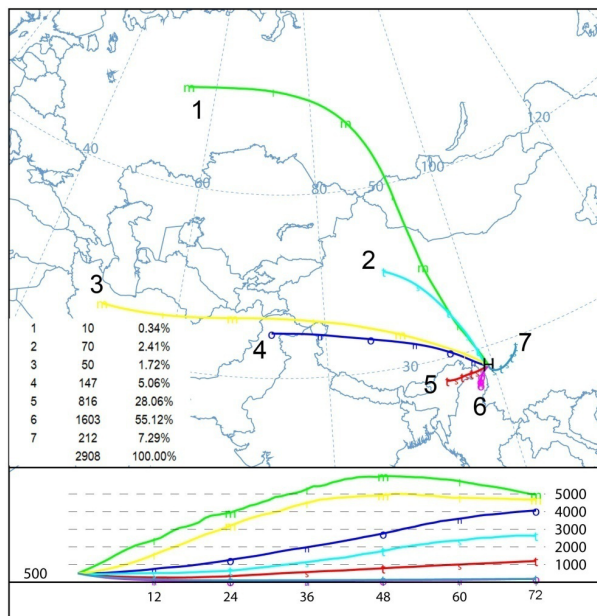


Fig. 4. Mean backward trajectories ending at Xianggelila. The endpoint height is 500 m.a.g.l. The numbers of trajectories in each cluster and their percent ratios among the total trajectories are shown. The unit of trajectory height is m.a.g.l.

Influence of airmass transport events on the variability of surface ozone

J. Ma et al.

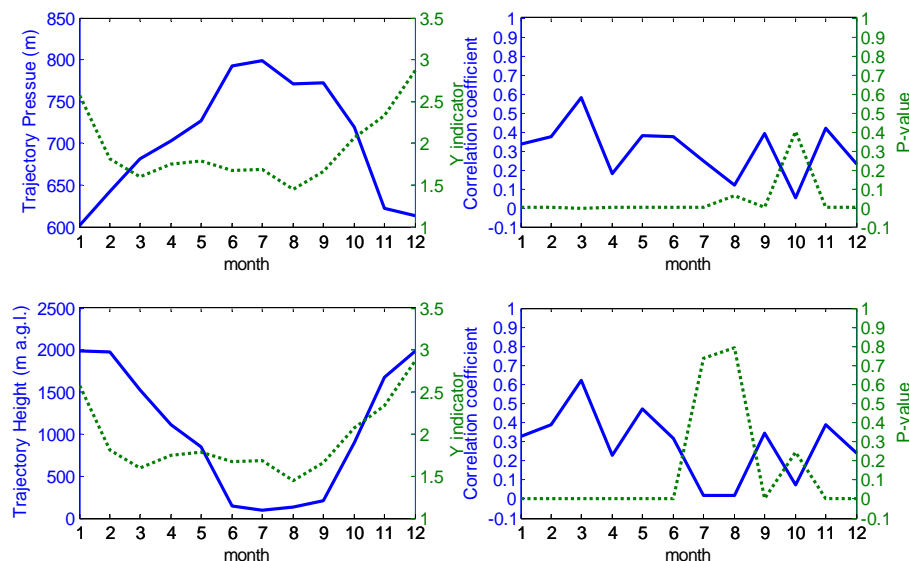


Fig. 6. Correlation between trajectory pressure level or height and Y indicator with significant levels (P value). The upper-left graph shows monthly trends of trajectory pressure and Y indicator, while the upper-right is the correlation between both. The lower-left graph shows monthly trends of trajectory height and Y indicator, while the lower-right is the correlation between both. Note that correlation between trajectory pressure and Y indicator is actually negative but shown in absolute value.

Title Page

Abstract

Introduction

Conclusions

References

Tables

Figures

◀

▶

◀

▶

Back

Close

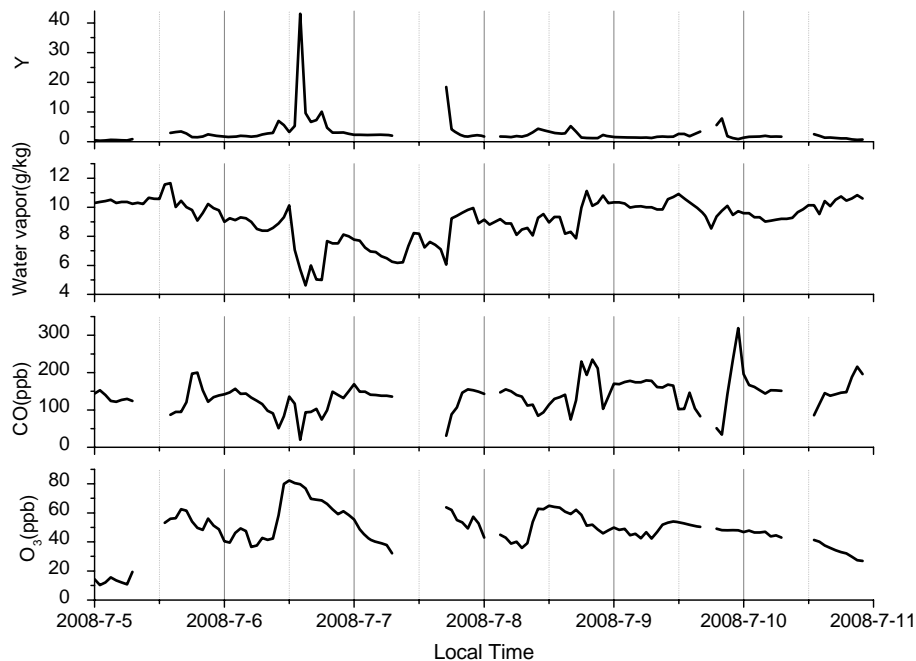
Full Screen / Esc

Printer-friendly Version

Interactive Discussion

Influence of airmass transport events on the variability of surface ozone

J. Ma et al.

**Fig. 7.** Time series of Y value, water vapor, CO and O₃ mixing ratios from 5 July to 11 July 2008.[Title Page](#)[Abstract](#)[Introduction](#)[Conclusions](#)[References](#)[Tables](#)[Figures](#)[⏪](#)[⏩](#)[◀](#)[▶](#)[Back](#)[Close](#)[Full Screen / Esc](#)[Printer-friendly Version](#)[Interactive Discussion](#)

Influence of airmass transport events on the variability of surface ozone

J. Ma et al.

Title Page

Abstract

Introduction

Conclusions

References

Tables

Figures

◀

▶

◀

▶

Back

Close

Full Screen / Esc

Printer-friendly Version

Interactive Discussion

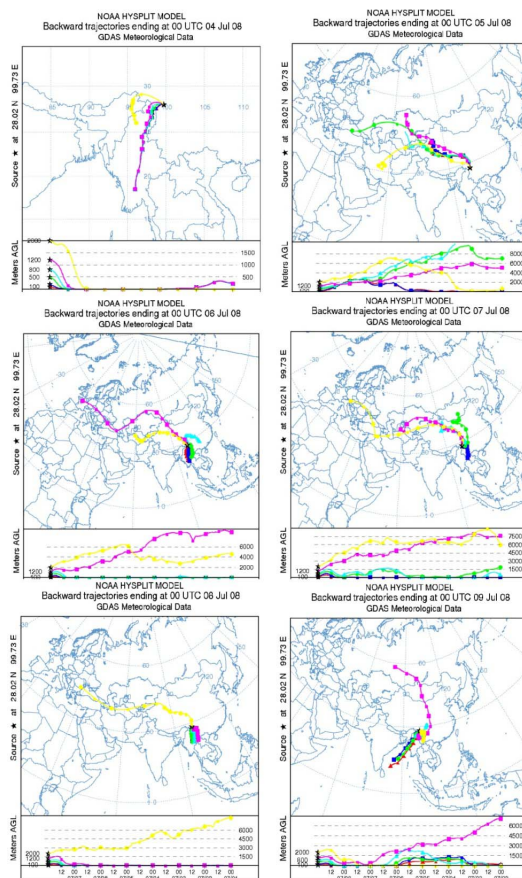


Fig. 8. Seven-day backward trajectories arriving at different heights over Xianggelila from 4 July to 9 July 2008.

Influence of airmass transport events on the variability of surface ozone

J. Ma et al.

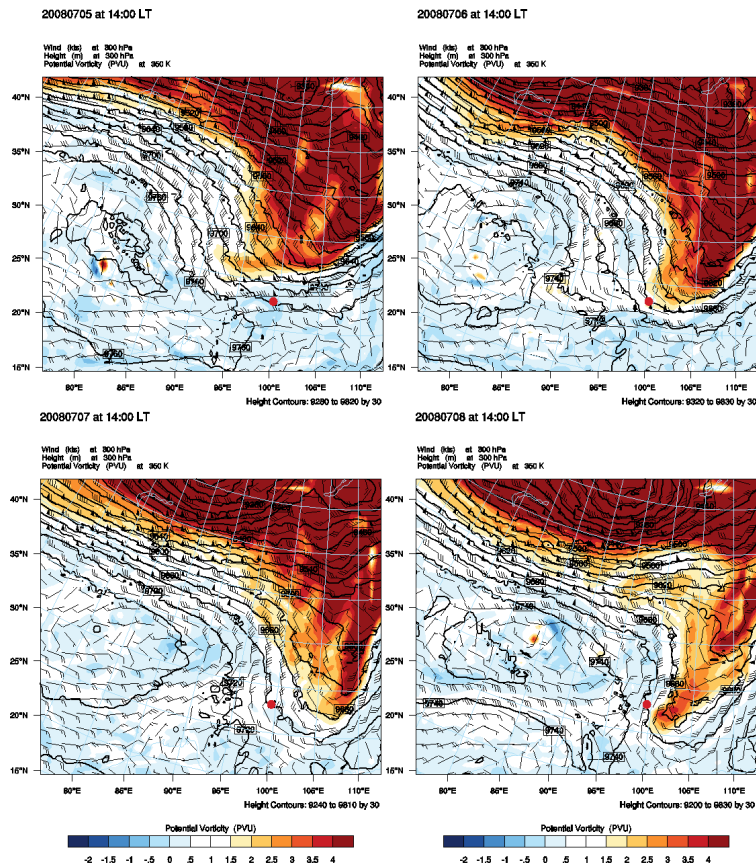


Fig. 9. Geopotential height, horizontal wind vector on 300 hPa and potential vorticity on 350 K from 5 July to 8 July 2008. The filled red circle denotes the Xianggelila station.

Title Page

Abstract Introduction

Conclusions References

Tables Figures

◀ ▶

◀ ▶

Back Close

Full Screen / Esc

Printer-friendly Version

Interactive Discussion



Influence of airmass transport events on the variability of surface ozone

J. Ma et al.

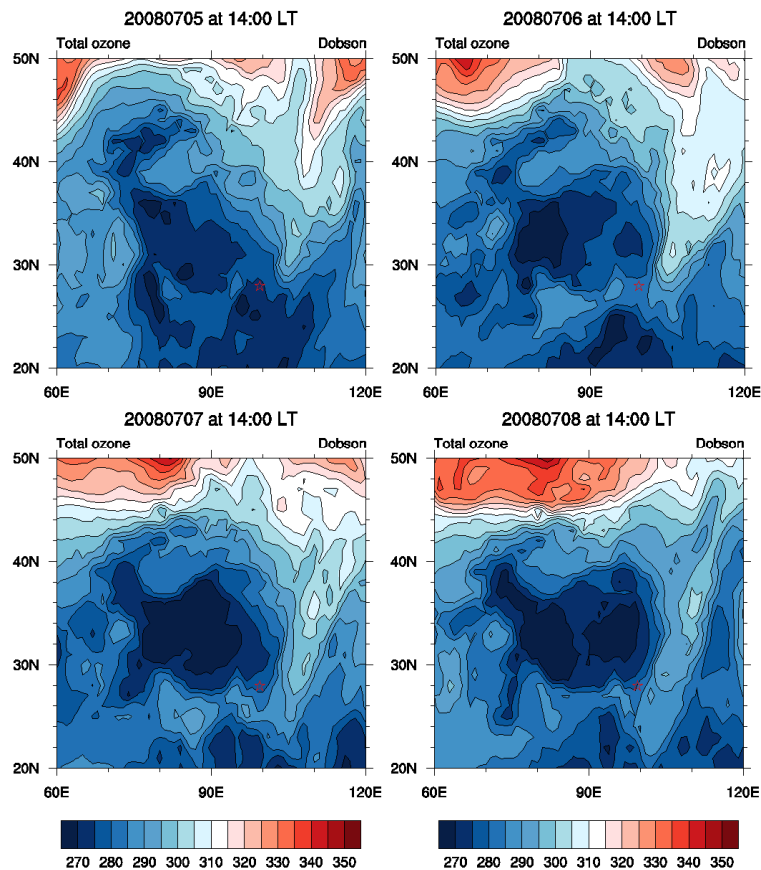


Fig. 10. Total column O_3 from 5 July to 8 July 2008. The red pentacle denotes the Xianggelila station.

Influence of airmass transport events on the variability of surface ozone

J. Ma et al.

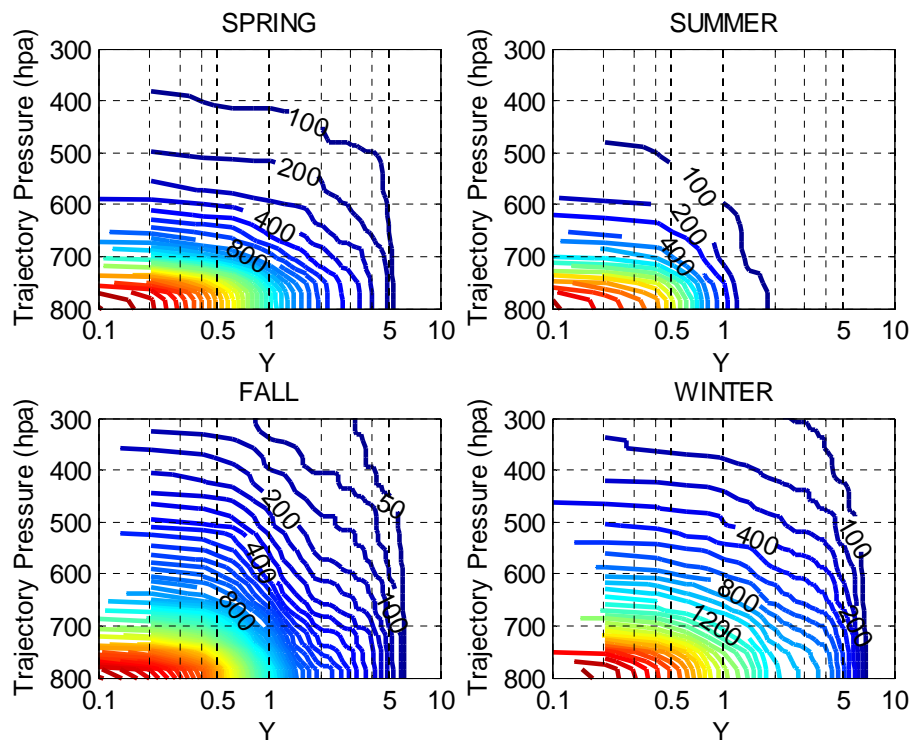


Fig. 11. Hours with both trajectory pressure lower than and Y value bigger than given values in different seasons. Note that x-axis is in logarithmic coordinate.

Title Page

Abstract

Introduction

Conclusions

References

Tables

Figures

⏪

⏩

⏴

⏵

Back

Close

Full Screen / Esc

Printer-friendly Version

Interactive Discussion

Influence of airmass transport events on the variability of surface ozone

J. Ma et al.

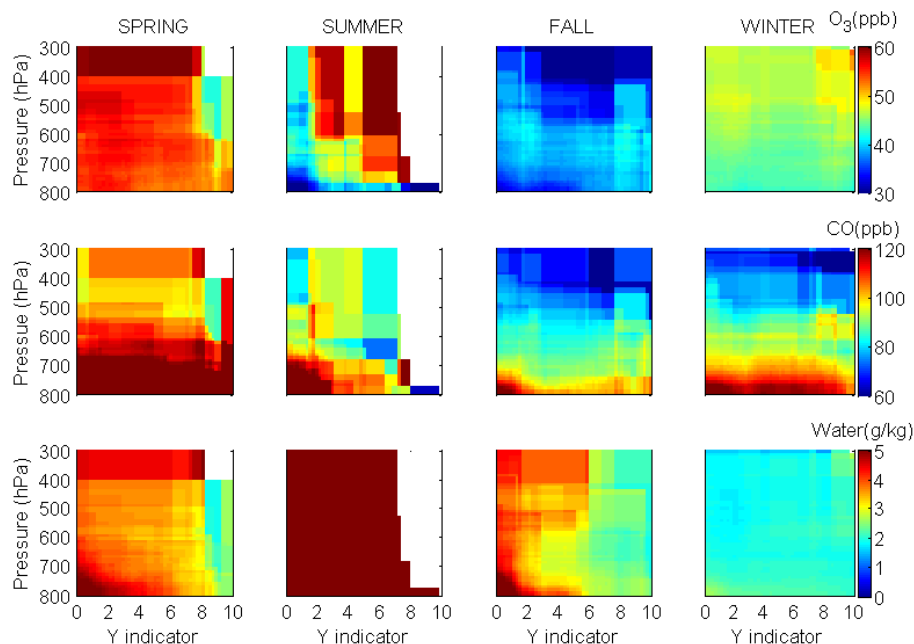


Fig. 12. Distributions of the values of O_3 , CO, and water vapor above specific trajectory pressure and Y indicator. Y-axis denotes trajectory pressure (hPa) and x-axis denotes Y indicator. Units of color bar of O_3 and CO are ppb; of water vapor is $g\,kg^{-1}$.

[Title Page](#)
[Abstract](#)
[Introduction](#)
[Conclusions](#)
[References](#)
[Tables](#)
[Figures](#)
[Back](#)
[Close](#)
[Full Screen / Esc](#)
[Printer-friendly Version](#)
[Interactive Discussion](#)